



Article

# Nanoemulsion Co-Loaded with XIAP siRNA and Gambogic Acid for Inhalation Therapy of Lung Cancer

Minhao Xu <sup>1,†</sup>, Lanfang Zhang <sup>2,†</sup>, Yue Guo <sup>1</sup>, Lu Bai <sup>1</sup>, Yi Luo <sup>1</sup>, Ben Wang <sup>1</sup>, Meiyan Kuang <sup>1</sup>, Xingyou Liu <sup>1</sup>, Meng Sun <sup>1</sup>, Chenhui Wang <sup>2</sup> and Jing Xie <sup>1,\*</sup>

<sup>1</sup> School of Pharmacy and Bioengineering, Chongqing University of Technology, Chongqing 400054, China

<sup>2</sup> Chongqing Key Laboratory of Natural Product Synthesis and Drug Research, Innovative Drug Research Center, School of Pharmaceutical Sciences, Chongqing University, 55 South Daxuecheng Road, Chongqing 401331, China

\* Correspondence: xiejing33@cqut.edu.cn; Tel.: +86-138-4300-4264

† These authors contributed equally to this work.

**Abstract:** Lung cancer is a leading cause of cancer mortality worldwide, with a 5-year survival rate of less than 20%. Gambogic acid (GA) is a naturally occurring and potent anticancer agent that destroys tumor cells through multiple mechanisms. According to the literature, one of the most potent inhibitors of caspases and apoptosis currently known is the X-linked Inhibitor of Apoptosis Protein (XIAP). It is highly expressed in various malignancies but has little or no expression in normal cells, making it an attractive target for cancer treatment. Here we report the development of a chitosan (CS)-based cationic nanoemulsion-based pulmonary delivery (p.d.) system for the co-delivery of antineoplastic drugs (GA) and anti-XIAP small interfering RNA (siRNA). The results showed that the chitosan-modified cationic nanoemulsions could effectively encapsulate gambogic acid as well as protect siRNA against degradation. The apoptosis analysis confirmed that the cationic nanoemulsions could induce more apoptosis in the A549 cell line. In addition, most drugs and siRNAs have a long residence time in the lungs through pulmonary delivery and show greater therapeutic effects compared to systemic administration. In summary, this work demonstrates the applicability of cationic nanoemulsions for combined cancer therapy and as a promising approach for the treatment of lung cancer.

**Keywords:** pulmonary delivery; co-delivery; RNAi; nanoemulsions; lung cancer



**Citation:** Xu, M.; Zhang, L.; Guo, Y.; Bai, L.; Luo, Y.; Wang, B.; Kuang, M.; Liu, X.; Sun, M.; Wang, C.; et al. Nanoemulsion Co-Loaded with XIAP siRNA and Gambogic Acid for Inhalation Therapy of Lung Cancer. *Int. J. Mol. Sci.* **2022**, *23*, 14294. <https://doi.org/10.3390/ijms232214294>

Academic Editor: Paola Manini

Received: 17 September 2022

Accepted: 15 November 2022

Published: 18 November 2022

**Publisher's Note:** MDPI stays neutral with regard to jurisdictional claims in published maps and institutional affiliations.



**Copyright:** © 2022 by the authors. Licensee MDPI, Basel, Switzerland. This article is an open access article distributed under the terms and conditions of the Creative Commons Attribution (CC BY) license (<https://creativecommons.org/licenses/by/4.0/>).

## 1. Introduction

As one of the most common malignant tumors in the world, lung cancer poses an enormous threat to human life and health [1]. Patients with early-stage lung cancer generally have no obvious symptoms, and most patients are already in the middle and late stages when detected, leading to poor treatment effects [2]. Currently, the main treatments for lung cancer are chemotherapy, radiotherapy, and surgery [3,4]. Although there have been some advances in diagnosis and treatment, the current shortage of effective first-line antitumor drugs, multidrug resistance of tumor cells [5], and unsatisfactory drug delivery methods [6,7] make improving the prognosis and survival rate of lung cancer patients much more difficult [7]. Consequently, the development of effective methods of treating lung cancer is imperative.

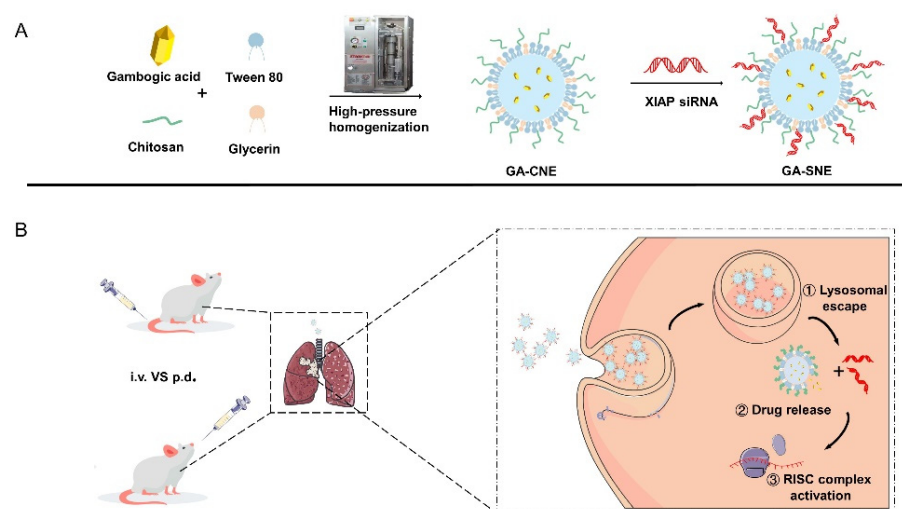
Traditional intravenous administration is a major obstacle to lung cancer treatment due to its inefficiency and side effects [8]. Compared to other administration routes, pulmonary delivery of drugs to treat lung diseases has clear advantages [7]. The accumulation of the drug in the lungs can be accelerated by topical administration [9,10]. Inhalation administration restricts the drug's ability to spread throughout the body, thus lowering systemic toxicity [6]. In most circumstances, inhalation medication delivery is superior to

oral or intravenous administration in terms of area under the curve (AUC), half-life, and drug concentration in the lungs [11].

Natural plant components are a significant source of chemotherapy medications and are thought to be less hazardous than the pharmaceuticals currently in use [12]. A naturally occurring anti-cancer substance known as gambogic acid (GA) is obtained from the *Garcinia cambogia* tree. In some malignancies, GA has been demonstrated to exhibit anti-angiogenic capabilities, antiproliferative effects, induce apoptosis, and reverse multidrug resistance (e.g., in breast and prostate cancer) [12,13]. Even though numerous *in vitro* and *in vivo* tests have indicated that gambogic acid has anticancer potential [14], its poor biodistribution, multiple targets, and low water solubility have restricted its practical applicability [13]. In earlier research, a variety of medication administration methods were used to increase GA utilization and lessen side effects. For the treatment of triple-negative breast cancer, Sang et al. described a redox/pH-responsive multifunctional composite magnetic micelle modified with hyaluronic acid that improved uptake into TNBC tumor cells, rapid drug release, and antitumor-enhanced tumor activity *in vivo* [15]. Liang et al. used hyaluronic acid to graft gambogic acid (HA-GA) and encapsulate the hydrophobic photosensitizer chlorophen Ce6 (Ce6) to prepare ROS-sensitive nanomicelles (HA-GA@Ce6). The results showed that the nanomicelles exhibit enhanced cellular uptake into 4T1 tumor cells and may produce greater anticancer efficacy by lowering intracellular antioxidant levels during tumor-specific triggered photodynamic therapy [16].

One of the most effective inhibitors of caspase and apoptosis found to date is the X-linked Inhibitor of Apoptosis Protein (XIAP) [17], which is also known to be critical for cell invasion, migration, and apoptosis [18,19]. It is an appealing target for cancer therapy since it is highly expressed in a variety of malignancies but is either absent or very poorly expressed in normal cells [17,20]. Many studies have demonstrated that antisense oligonucleotides or small interfering RNA (siRNA) can suppress tumor cell proliferation, cause apoptosis, and make tumor cells more sensitive to chemotherapeutic treatments by inhibiting XIAP expression [21,22]. At the moment, simultaneous delivery of nucleic acids and cancer-fighting medications via a single nanoparticle platform offers good therapeutic benefits [23,24]. In this scenario, systemic toxicity and the dose of cancer treatment would be reduced. Additionally, combination therapies created through the concurrent administration of anticancer medications and nucleic acids may have therapeutic benefits that are additive or synergistic [25]. As a result, the combination of GA and XIAP inhibition is a promising lung therapy for lung cancer.

In this study, we designed cationic nanoemulsions for the simultaneous delivery of siRNA and gambogic acid. Nanoemulsions increased the solubility of gambogic acid, and chitosan, a naturally occurring cationic polymer, was employed to coat the nanoemulsions' surface. Chitosan can also interact electrostatically with siRNA to produce electrostatic complexes that increase the stability of siRNA *in vivo* and the effectiveness of cellular uptake (Scheme 1A). Hence, using pulmonary administration and systemic injection, respectively, to transport the drug-loaded system into the lungs of lung cancer model mice, the biodistribution of the cationic nanoemulsions and the effectiveness of lung tumor inhibition were assessed (Scheme 1B).



**Scheme 1.** Schematic diagram of nanoemulsions co-loaded with gambogic acid and XIAP siRNA for lung cancer treatment. The cationic nanoemulsions (GA-CNE) were prepared by a high-pressure homogenizer. The prepared nanoemulsions were incubated with siRNA at room temperature to prepare co-loaded nanoemulsions (GA-SNE) (A) by pulmonary administration or tail vein injection, compared with its anti-tumor effect in vivo. After entering the body, GA-SNE is taken up by tumor cells, detached from lysosomes by the proton sponge effect, and releases the drug in the cells, achieving antitumor effects of gambogic acid and gene silencing (B).

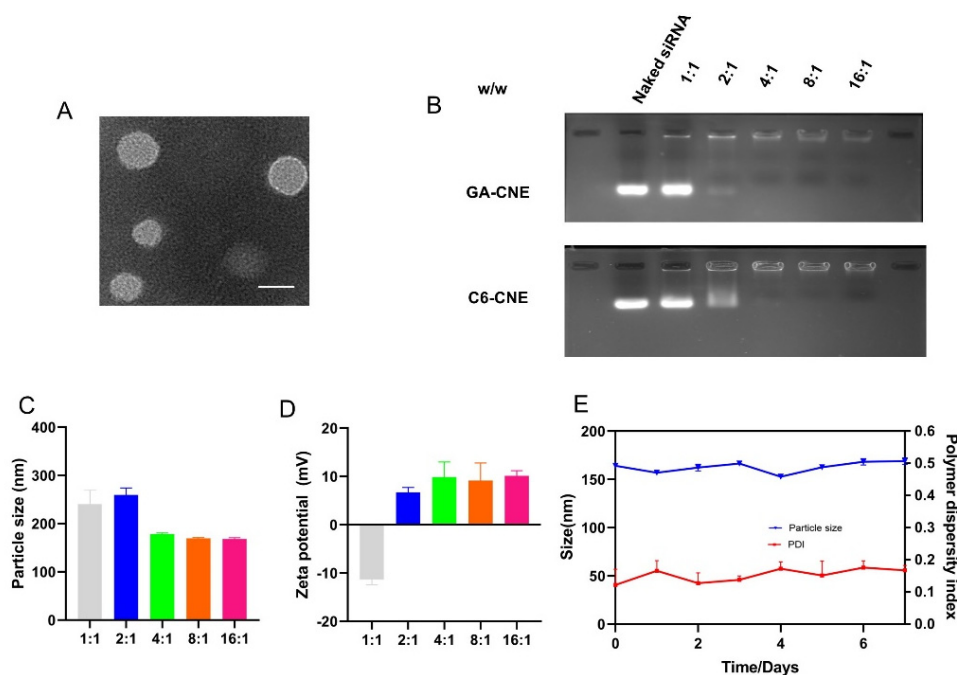
## 2. Results

### 2.1. Preparation and Characterization of Nanoemulsions

By using dynamic light scattering (DLS), cationic nanoemulsions' mean particle sizes were determined to be  $183.81 \pm 1.15$  nm, with a PDI of  $0.210 \pm 0.013$  (Table 1). The size and PDI of the cationic nanoemulsions were altered to  $174.53 \pm 0.78$  nm and  $0.262 \pm 0.014$ , respectively, after loading GA. In the transmission electron microscope (TEM), the emulsions appeared as regular spherical structures (Figure 1A) with a zeta potential of  $9.93 \pm 0.58$  mV for the GA-CNE (Table 1). Since the nanoemulsions had a good solubilizing effect on insoluble drugs, the prepared nanoemulsions had a drug encapsulation rate as high as  $91.51 \pm 3.732\%$  (Table 1). To study drug uptake in cells, C-6 (coumarin-6) was used as a fluorescent probe, and its particle size, potential and PDI were characterized (Table 1). To create GA-SNE, siRNA and GA-CNE were combined in varying quantities, and a laser particle size analyzer was used to determine the average particle size and zeta potential of the mixture. Figure 1C, D displays the results. The figure shows that when GA-CNE and siRNA were combined at a volume ratio of 1:1, the positive charge of chitosan was neutralized by the negative charge of siRNA, resulting in a zeta potential of  $-11.37 \pm 0.62$  mV and an increase in particle size. This might be the result of the system becoming unstable, since there was not enough chitosan in GA-CNE to completely load all of the siRNAs. The charge of GA-CNE returned to positivity as the volume rose, and the particle size likewise tended to stabilize. The same procedures were used to prepare GA-SNE with various weight ratios, and agarose gel retardation electrophoresis was used to determine the degree of binding between GA-SNE and siRNA. Figure 1B presents the findings. The graphic shows that free siRNA migrates during electrophoresis, and the band gradually darkens as the  $w/w$  value rises. There is no band in the lane when the GA-CNE: siRNA  $w/w$  value is 4. The bands and brightness are entirely focused in the dotted wells, showing that GA-CNE can completely bind to siRNA when GA-CNE: siRNA  $w/w = 4$ . C6-CNE was subsequently characterized according to the same conditions and showed similar results (Figure 1B). Additionally, we looked into the carrier's stability. As seen in Figure 1E, GA-CNE maintained a constant size and PDI, which supported the carrier's strong stability.

**Table 1.** Particle Size, Zeta Potential, PDI, and Encapsulation Efficiency of Nanoemulsions (Mean  $\pm$  SD,  $n = 3$ ).

Nanoparticles	Particle Size (nm)	PDI	Zeta Potential (mV)	Encapsulation Efficiency (%)
CS-CNE	183.81 $\pm$ 1.15	0.210 $\pm$ 0.013	12.37 $\pm$ 0.75	N
GA-CNE	174.53 $\pm$ 0.78	0.262 $\pm$ 0.014	9.93 $\pm$ 0.58	91.51 $\pm$ 3.732
C6-CNE	174.26 $\pm$ 1.15	0.280 $\pm$ 0.011	15.57 $\pm$ 0.37	N

**Figure 1.** Characterization of CNE. (A) GA-SNE transmission electron micrograph. Scale bar: 200 nm. (B) Agarose gel retardation assay at varying GA-CNE/siRNA *w/w* ratios. (C) Particle size and (D) zeta potential of varying GA-CNE/siRNA. (E) Stability of GA-CNE in PBS.

## 2.2. Cellular Uptake

Coumarin-6 was employed as a fluorescent probe to examine how GA-SNE is absorbed by cells, and A549 cells were given GA-SNE, free siRNA, or GA-CNE treatments, as appropriate. Flow cytometric analysis and confocal microscopy were utilized to measure the levels of various formulations integrated into the A549 cells after 4 h of incubation. Due to the positive charge and tighter size distribution, GA-CNE demonstrated a significant level of cellular absorption. The fact that GA-SNE was substantially more readily absorbed as compared to free siRNA absorption suggests that cationic nanoemulsions can bind to and safeguard siRNA. Further confirmation of such results was obtained using flow cytometry (Figure 2B,C). Once the siRNA enters the cell, it must exit the lysosome to post-transcriptionally silence cytoplasmic genes. By labeling the cell nucleus with 4-diamidino-2-phenylindole and the lysosomes with LysoTracker Green, the co-staining experiment was further carried out to investigate the endosomal escape of siRNA. As can be seen, free siRNA (red) colocalized with lysosomes (green), while part of the red fluorescence from GA-SNE started to dissociate from the green fluorescence (Figure 2D), implying that the siRNA started to migrate to escape from the lysosome. Results showed that GA-SNE successfully escaped endosomes and effectively delivered siRNA.

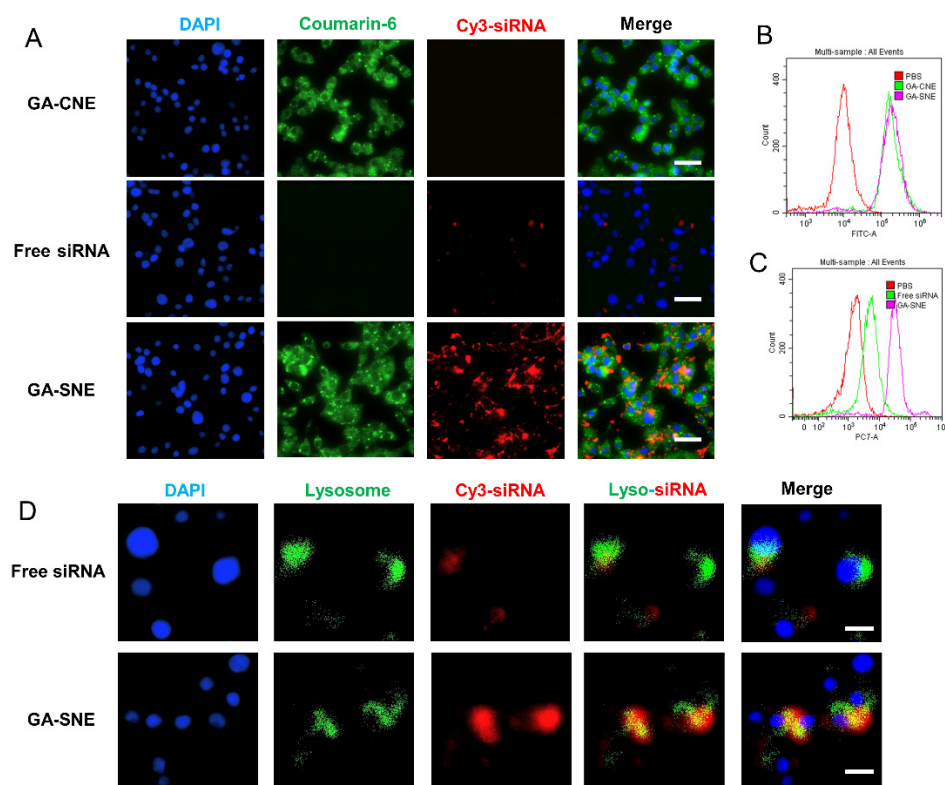


**Figure 2.** Cellular uptake of GA-CNE. (A) Confocal laser scanning microscopy (CLSM) images of cellular uptake with different treatments after 4 h. Scale bar: 50  $\mu$ m. (B) Cellular uptake of GA and (C) siRNA after 4 h of incubation was analyzed by flow cytometry. (D) Confocal laser scanning microscopy (CLSM) images of lysosomal escape with different treatments after 4 h. Scale bar: 20  $\mu$ m.

### 2.3. Cell Viability

In A549 cells, the ratio of GA to XIAP siRNA in GA-SNE was optimized. A549 proliferation was significantly inhibited by GA-SNE with a GA/siRNA ratio of 1:3 (Figure 3A). This ratio, therefore, was chosen for subsequent tests. A549 cells were treated with CS-CNE, CS-SNE, GA-CNE, and GA-SNE, respectively, to test the preparations' *in vitro* anticancer effects. Cell viability was assessed using the CCK-8 cytotoxicity assay. Neither GA-CNE nor siRNA had a significant inhibitory effect on the cells. GA-SNE, on the other hand, showed the highest inhibitory effect among all groups (Figure 3B), indicating that the co-delivery system delivering siRNA and GA simultaneously would have a synergistic inhibitory effect on cells *in vitro*.

### 2.4. Analysis of Apoptosis and Cell Cycle Arrest

Using Annexin V-FITC labeling, apoptosis caused by GA and XIAP siRNA was identified. The untreated control cells showed a comparatively low percentage of apoptosis (0.71%), as illustrated in Figure 3C. Furthermore, consistent with CCK8 results, cells incubated in the GA-SNE group underwent up to 94.53% apoptosis compared to CS-SNE, 78.12% higher than the effect of CS-SNE. These results suggest that GA and XIAP siRNA can promote A549 cell death by inducing apoptosis. Following treatment with various preparations, flow cytometry was used to identify the A549 cell cycle. Our results (Figure 3D,E) showed that GA and XIAP alone led to cell cycle G0/G1 arrest, similar to those previously reported [26,27]. Encouragingly, A549 cells were more frequently arrested in the G0/G1 phase in the combination group. These results suggested that by altering the cell cycle, our formulation can prevent tumor cells from proliferating.

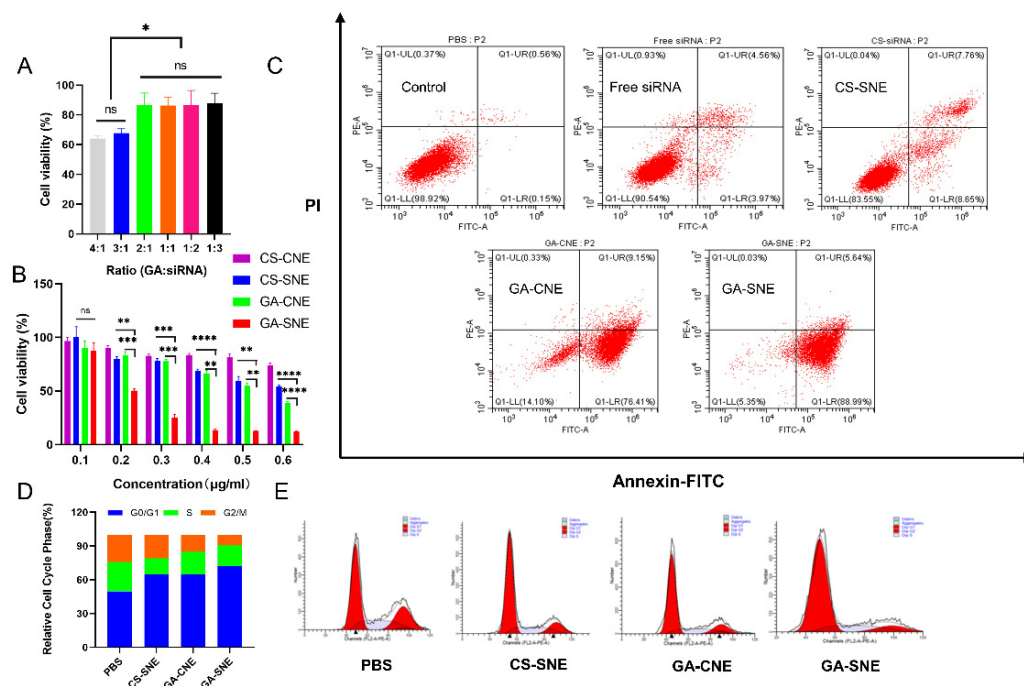


**Figure 3.** Effects of GA on cancer cells. (A) Cell viability of A549 cells after incubation with GA-SNE with different GA/siRNA ratios. (B) In vitro cell viability of A549 cells following incubation with CS-CNE, CS-SNE, GA-CNE, and GA-SNE nanoemulsions for 24 h, respectively. (C) A549 cells were treated with different formulations, and cell apoptosis was detected by flow cytometry. (D) Cell cycle quantification is treated with different preparations. (E) A549 cells were employed with different formulations for 24 h. The cell cycle was evaluated by flow cytometry (the value bars with ns are not significant, \*  $p < 0.05$ , \*\*  $p < 0.01$ , \*\*\*  $p < 0.001$ , \*\*\*\*  $p < 0.0001$ ).

### 2.5. Western Blot

A549 cells were treated with naked siRNA, CS-SNE, and GA-SNE, respectively, to further assess the gene interference effectiveness of siRNA-loaded nanoemulsions in vitro. Results from Western blotting revealed that both CS-SNE and GA-SNE dramatically decreased the expression of XIAP protein in A549 cells when compared to control and naked siRNA (Figure 4A). This indicates that chitosan as a cationic shell protects siRNA well and increases its stability. It has been demonstrated that GA-SNE has an in vitro gene interference effect. ImageJ was used to quantify the data, and the results demonstrated that siRNA could be successfully encapsulated in the cationic nanoemulsions for in vitro gene silencing (Figure 4B).

### 2.6. Biodistribution

Using tracheal instillation or intravenous injection, the in vivo imaging system tracked the distribution of Cy3-siRNA-loaded nanoemulsions in various organs at various periods. One hour after administration, the majority of the drug's concentration in the p.d. group was in the lungs, whereas the i.v. injection group's GA-SNE showed less lung accumulation and more accumulation at the renal site. At 12 and 24 h, the i.v. group showed negligible lung distribution, and the majority of the fluorescence was found in the liver and kidney (Figure 5B), indicating that most of the siRNA in the iv group was blocked by the kidneys and cleared quickly. In contrast, the p.d. group retained a significant amount of siRNA in the lungs at 12 and 24 h.

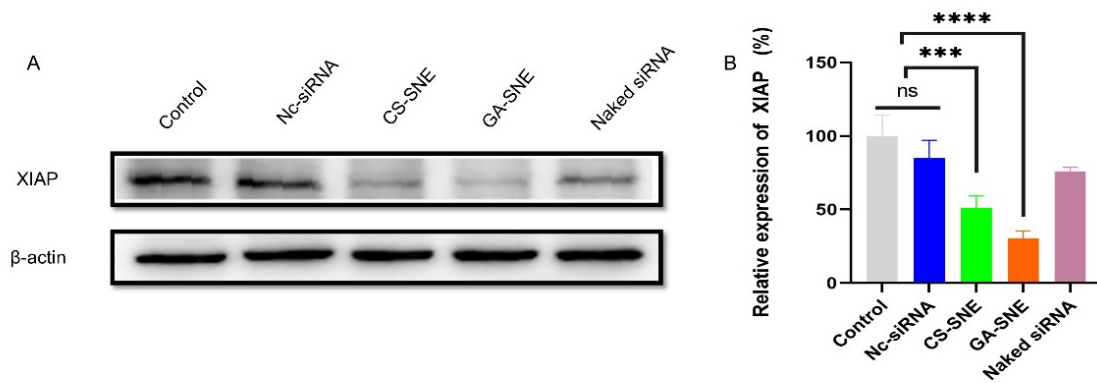


**Figure 4.** Effect of GA-CNE on XIAP protein expression. (A) Western blot analysis of XIAP protein in A549 cells treated with different formulations. (B) ImageJ quantification of the relative expression rate of XIAP protein in vitro (the value bars with ns are not significant, \*\*\*  $p < 0.001$ , \*\*\*\*  $p < 0.0001$ ).

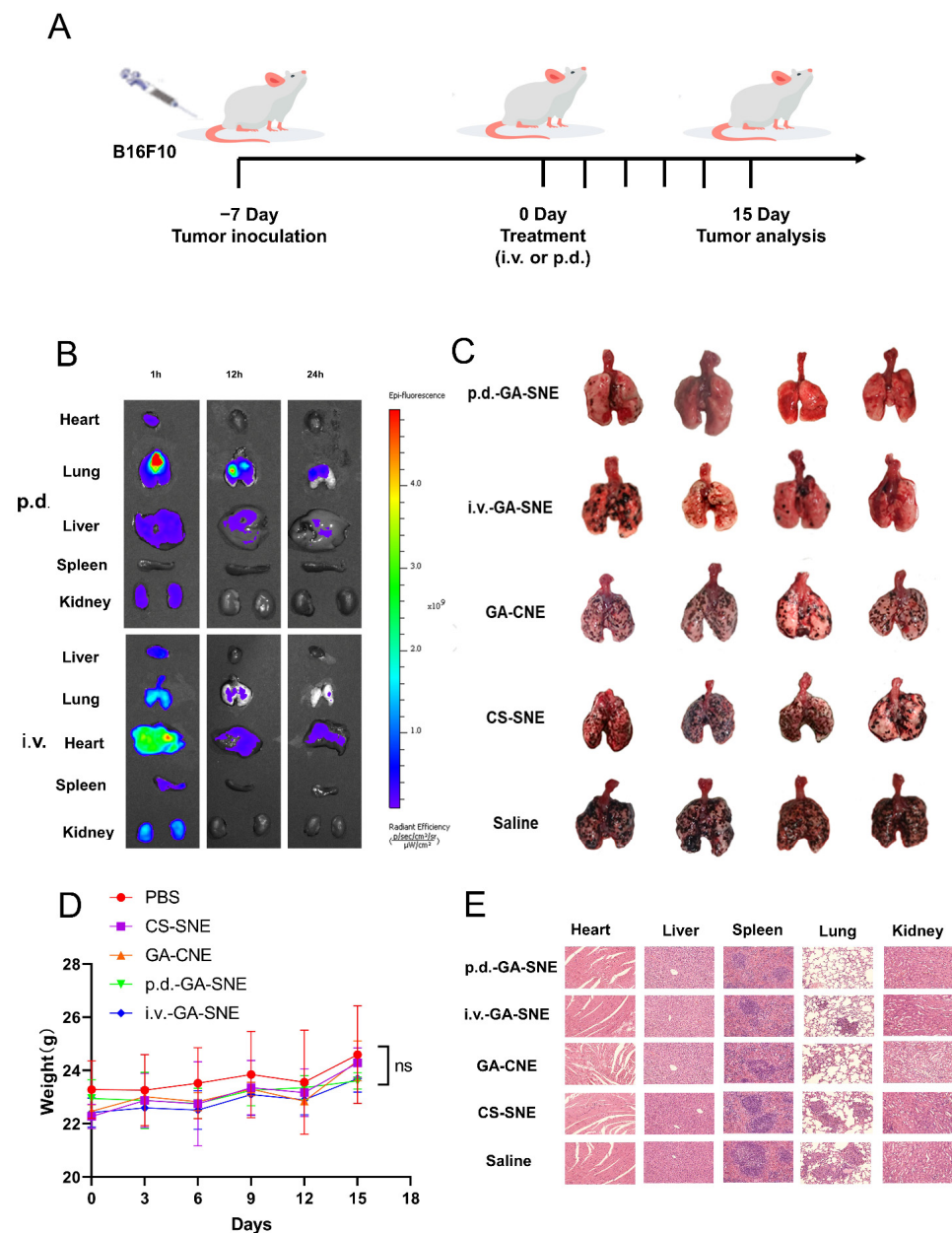


**Figure 5.** In vivo efficacy of GA-CNE in a murine tumor model. (A) Schedules for treatment and analysis. An animal model of lung cancer was created by injecting B16F10 cells ( $1.5 \times 10^6$  cells per

mouse) into female BALB/c mice (18–20 g). Treatments were administered either by pulmonary delivery or by tail-vein injection on days 7, 9, 11, and 13 for a total of four doses. Mice were euthanized on day 15, and lungs and other organs were removed for analysis. **(B)** Ex vivo Cy3-siRNA fluorescence images of major organs after p.d. or i.v. administration. From top to bottom: heart, lung, liver, spleen, and kidneys. **(C)** Photographs of lungs obtained from BALB/c mice. **(D)** Changes in body weights of the mice ( $n = 4$ ). **(E)** Histological sections of heart, liver, spleen, lung, and kidney organs of BALB/c mice after different treatments. Scale bar: 100  $\mu\text{m}$ .

### 2.7. The Codelivery System's In Vivo Therapeutic Effectiveness

The antitumor efficacy of the drug in combination with XIAP siRNA was investigated in Balb/C mice with lung cancer. Every three days, the body weight of each mouse was recorded during the animal experiment (Figure 5D), and there was no significant change in body weight in any group, implying the safety of the delivery system and treatment method. Pictures of the lungs taken from Balb/C mice in various treatment and control groups are shown in Figure 6C. In the lungs of B16F10 melanoma-bearing mice treated with the PBS group, there were numerous melanoma lymph nodes, and the tumor practically filled the entire lung. Significantly, compared to the PBS group or the single delivery method, the lungs of mice treated with the co-delivery system displayed fewer tumor nodes. Additionally, the GA-SNE p.d. group had fewer and smaller lung nodules than the GA-SNE intravenous therapy group, demonstrating the superiority of p.d.

### 2.8. Histopathological Examination

Hematoxylin and eosin (H&E) staining was used to further confirm anticancer efficacy. Comparing the groups that received PBS or the single delivery system, significant tumor nodules were seen in the lungs; however, in the co-delivery system, tumor mass and number were significantly reduced, and numerous normal pores were visible. The major organs of mice treated with GA-CNE, CS-SNE, and GA-SNE also showed little obvious pathology when stained with H&E compared to animals treated with PBS (Figure 5E), which demonstrated the high biocompatibility and biosafety of the nanoemulsions.

### 2.9. TUNEL Assay and Immunohistochemistry

Using the TUNEL assay, the induction of apoptosis in model mice was further studied. Compared to the control group and the single drug groups, the co-administration system dramatically increased the number of apoptotic cells in the tumor tissue (Figure 6A). According to IHC analysis, the primary biochemical marker of tumor growth, Ki67, was found to be highly expressed in both the control and single drug groups. However, GA and siRNA treatment significantly reduced the expression of Ki67 in tumor tissue, showing greater anticancer effects than other groups (Figure 6B). The data above demonstrate that the combined administration group could achieve significant antitumor efficacy by inducing cell apoptosis and inhibiting cell proliferation in comparison to the PBS or single administration groups.

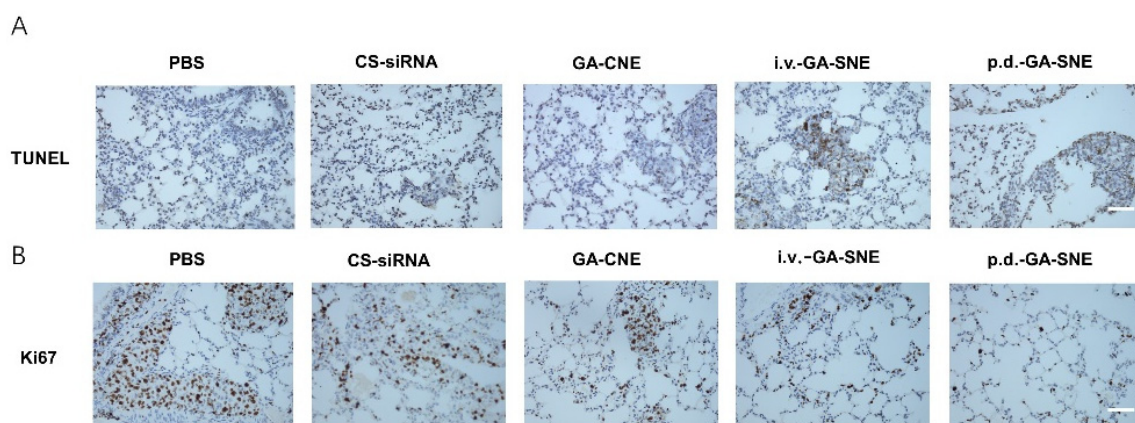


**Figure 6.** Analysis of murine tumor model treated with GA-CNE. (A) TUNEL analysis in the tumor region slices after all treatments. Scale bar: 100 µm (B) IHC analysis of Ki67 in the tumor region slices after all treatments. Scale bar: 100 µm.

### 3. Discussion

At present, nanoparticles show promise for inhalation drug delivery from the lung in the treatment of lung diseases. We successfully constructed a cationic nanoemulsion platform to achieve combined GA and siRNA therapy. However, pulmonary inhalation of nanoparticles is prone to receive clearance by mucous cilia in the lung, which affects the efficiency of drug pulmonary delivery, so it is necessary to further consider the movement and deposition of nanoparticles in the lung. In addition, the large surface area and rich vascularity of the lung lead to differences in the pharmacokinetics of the drug compared to systemic administration, so further studies are needed to investigate differences in drug metabolism due to differences in the two modes of administration. In addition, the toxicity of excipients is also a factor that should be considered for the safety of nanoformulations for inhalation administration. The excipients and carrier materials involved in the preparation process may lead to unintended adverse reactions, and therefore, for the application of nanoformulations to the lung, the potential pulmonary toxicity issues that may exist must be considered.

Therefore, to better enable pulmonary delivery of GA and siRNA combination therapy in clinical practice, more thorough studies are needed to optimize the composition, particle size, preparation methods, drug metabolism kinetics, inhalation loading compatibility and excipient safety of cationic nanoemulsions. These efforts will help to overcome the challenges of pulmonary delivery.

### 4. Materials and Methods

#### 4.1. Materials

Gambogic acid was purchased from Sigma-Aldrich (St. Louis, MO, USA). Cy3-labeled siRNA (XIAP siRNA) was purchased from RiboBio (Guangzhou, China) with the following sequences: XIAP siRNA (sense): 5-AAG UGG UAG UCC UGU UUC AGC-3. Monoclonal antibodies (XIAP) and HRP-linked antibodies were purchased from Cell Signaling Technology (Danvers, MA, USA). Cell Count Kit-8, 4',6-diamidino-2-phenylindole (DAPI), and LysoTracker Green were from the Beyotime Institute of Biotechnology (Shanghai, China). Annexin V-FITC Apoptosis Detection Kit and Cell Cycle and Apoptosis Detection Kit were from Beijing Biotopped Technology Co., Ltd. (Beijing, China). Tween-80, squalene, and glycerol were manufactured by Shanghai Energy Chemical Co., Ltd. Immunohistochemistry Kit (D601037-0050) was purchased from Sangon Biotech (Shanghai, China). Deionized water was produced in the laboratory. The reagent-grade chemicals used in the tests were all used exactly as provided to the researchers.

#### 4.2. Cell Culture and Animal Care

A549 cells were bought from ATCC and grown in DMEM with 10% FBS supplement. All cells were kept in an incubator at 37 °C with 5% CO<sub>2</sub>. Fetal bovine serum (FBS), Trypsin and DMEM were bought from Hyclone (Logan, UT, USA). BALB/c female mice (18–20 g), 6–8 weeks old, were purchased from Byrness Weil Biotech Ltd. (Chongqing, China). The Chongqing University of Technology Experimental Animal Ethics Committee developed standards for laboratory animal care, which were followed in all animal research.

#### 4.3. Preparation and Characterization of Nanoemulsions

By using a high-energy emulsification technique, nanoemulsions were created. To prepare the water phase, Tween 80 and glycerol (4:1, volume ratio) were added to PBS, while the oil phase was created by dissolving gambogic acid in a small amount of ethanol and combining it with squalene. Then, a coarse emulsion was prepared by gradually adding the oil phase while stirring continuously. Then, to prepare nanoemulsions (GA-NE), we homogenized the prepared coarse emulsion using a high-pressure homogenizer (Homogenizing Systems Ltd., Harlow, UK). We set the pressure setting to 100 Mpa and homogenized for a total of 10 cycles. The aqueous phase of the cationic nanoemulsions (GA-CNE) was supplemented with an additional 1% hydrochloric acid chitosan (70–90% deacetylation degree), and the remaining processes remained the same. C6-CNE was prepared by replacing GA with C6, and the rest of the process remained the same. The NanoBrook 90Plus PALS Zetasizer (Brookhaven, NY, USA) and transmission electron microscopy (TEM) (Hitachi, Japan) were used to determine the surface charge, size, and morphology of GA-CNE, respectively. Every day for 7 days at 37 °C, the changes in particle size and the polydispersity index (PDI) of GA-CNE in PBS were monitored to evaluate the stability. The amount of encapsulated GA in GA-CNE was measured at 360 nm using HPLC. The following equations were used to calculate the encapsulation efficiency:

$$\text{Encapsulation rate(\%)} = \frac{\text{The content of gambogic acid in nanoemulsions}}{\text{Dosage of gambogic acid}} \times 100\% \quad (1)$$

#### 4.4. Preparation and Characterization of GA-SNE

To load XIAP-siRNA onto GA-CNE (GA-SNE), siRNA solutions (20 µM) were put into GA-CNE solutions at 1:1, 2:1, 4:1, 8:1, and 16:1 with *w/w* ratios of GA-CNE/siRNA and left at room temperature for 30 min. The development of the GA-CNE/siRNA complex was then verified using a gel retardation experiment employing 2% agarose gel and 100 V voltage for 15 min. The complexes' size and zeta potential were determined using a NanoBrook 90Plus PALS Zetasizer (Brookhaven, NY, USA).

#### 4.5. Cellular Uptake

Coumarin-6 was employed as the fluorescent probe and  $5 \times 10^4$  A549 cells were used to examine the uptake effect of nanoemulsions. In a 24-well plate, A549 cells were cultivated for the night. For 4 h, cells were exposed to 50 nM free Cy3-siRNA, GA-CNE (containing 0.05 µg/mL Coumarin-6), and GA-SNE (containing both 50 nM siRNA and 0.05 µg/mL Coumarin-6). After three PBS washes, the samples were fixed with paraformaldehyde (4%) for 10 min, stained with DAPI (2 µg/mL) for 10 min to highlight the cell nuclei, and then rewashed three times with PBS. A confocal laser scanning microscope (CLSM) was used to measure how well the nanoemulsions were internalized by the cells (Nikon, Japan).

##### 4.5.1. Quantitative Cell Uptake

The internalization of different agents in A549 cells was quantitatively evaluated by flow cytometry. Briefly, 24-well plates with  $5 \times 10^4$  A549 cells were planted and cultured at 37 °C for 24 h. After that, the culture medium was replaced with fresh medium containing Cy3-labeled siRNA, GA-CNE, and GA-SNE. After 4 h, the medium was withdrawn, and the cells were trypsinized, centrifuged, twice-washed in PBS, and then resuspended in

500 mL PBS for CytoFLEX FCM analysis (Beckman Coulter Corp., Brea, CA, USA). The control group consisted of cells that received no treatment.

#### 4.5.2. Endosomal Scape

The method used to prepare the samples for this study was the same as that described in Section 4.5 for cellular uptake. LysoTracker Green was used to label A549 cells after they had been exposed to the material for 4 h at 37 °C. For this, cells were given 50 nM of the dye diluted in DMEM, and it was left in place for 30 min. Following the removal of the dye, the cells underwent three PBS washes. The cells were then labeled with DAPI, fixed with 4% paraformaldehyde, and examined under confocal microscopy.

#### 4.6. Cell Viability

A549 cells ( $1 \times 10^4$  cells/well in a 96-well plate) were treated with GA-SNE with various molar ratios of GA: XIAP siRNA (3:1, 2:1, 1:1, 1:2, and 1:3) to optimize the ratio of GA and XIAP siRNA in GA-SNE. About  $1 \times 10^4$  A549 cells were grown in fresh media with various formulations and incubated at 37 °C with 5% CO<sub>2</sub> to determine the toxicity of the samples. After 24 h, the samples were incubated for 4 h with a 10% CCK8 reagent in place of the culture medium. Utilizing a microplate reader to measure absorbance at 450 nm, the percentage of relative cell viability was calculated in comparison to that of the negative control (cells treated with PBS). For this test, four groups were used: GA-CNE (GA = 0.1–0.6 µg/mL), GA-SNE (GA = 0.1–0.6 µg/mL, ratios of GA: XIAP siRNA = 3), CS-SNE (with an equivalent amount of siRNA as GA-SNE) and CS-CNE (with an equivalent amount of chitosan as GA-CNE).

#### 4.7. Evaluation of Cell Cycle Arrest and Apoptosis

Using the Cell Cycle and Apoptosis Analysis Kit (Top0232-50T, Biotopped, Beijing, China) and the ANNEXIN V-FITC/PI Apoptosis Assay Kit (TOP2210-100, Biotopped, Beijing, China), respectively, flow cytometry analysis was used to examine the induction of cell cycle arrest and apoptosis. About  $5 \times 10^4$  A549 cells were grown in a 24-well plate and incubated for 24 h at 37 °C. Fresh culture medium containing free siRNA, CS-SNE, GA-CNE, and GA-SNE was then used to treat the cells. The GA and XIAP siRNA doses per well were 0.3 µg/mL and 50 nM, respectively. After being incubated for 24 h, the cells were rinsed with PBS, collected, and resuspended in 500 L of binding buffer, then stained following the instructions provided with the apoptosis detection kit. Then, using flow cytometry, the fluorescence intensity of the labeled cells was evaluated. Cells were collected and preserved with 70% ethanol at –20 °C for the duration of the cell cycle test. Cells were stained for 5 min with PI and examined with a CytoFLEX FCM (Beckman Coulter Corp., Brea, CA, USA).

#### 4.8. Western Blot

After being plated into a 6-well plate, about  $5 \times 10^6$  A549 cells were left to incubate overnight. Following a PBS wash, the transfection method using various formulations was carried out as previously mentioned. Total protein was then extracted after 24 h, separated using SDS-PAGE, transferred to a nitrocellulose membrane, probed with XIAP antibodies, and then incubated for a final hour at 37 degrees Celsius with an HRP-linked secondary antibody (actin was used as a housekeeping control).

#### 4.9. Lung Cancer Induction in BALB/c Mice

The Animal Experimentation Ethics Committee at Chongqing University developed standards for laboratory animal care, which were followed in all animal research. An animal model of lung cancer was created by injecting B16F10 cells ( $1.5 \times 10^6$  cells per mouse) into female BALB/c mice (18–20 g).

#### 4.10. Biodistribution

GA-SNE (GA = 3 mg/kg, molar ratios of GA: XIAP siRNA = 3) was administered to mice either intravenously or by pulmonary delivery. Mice were sacrificed, and their primary organs—their hearts, lungs, livers, spleens, and kidneys—were removed at 0, 12, and 24 h after injection. An *in vivo* imaging system was used to investigate the fluorescence distribution following PBS washing (PerkinElmer, Waltham, MA, USA).

#### 4.11. *In Vivo* Antitumor Therapy

Twenty female BALB/c mice (18–20 g) in total were distributed into five groups of four at random. Four doses of treatment were given on days 7, 9, 11, and 13, either by pulmonary administration or by tail-vein injection. For the pulmonary administration, the mice were administered the formulations (GA = 3 mg/kg, molar ratios of GA: XIAP siRNA = 3) in a volume of 25 L in PBS by intratracheal instillation after they had been given general anesthesia. Tail-vein injection used the same volume and concentration of the drug.

#### 4.12. Histological Examination

Lung specimens were fixed with paraformaldehyde (4%), embedded in paraffin, sectioned, and stained with hematoxylin and eosin (H&E). For histopathological observations to further assess the *in vivo* safety of various formulations, other organs (hearts, livers, spleens, and kidneys) were collected from each group of mice, stained with H&E, and assessed by microscopy.

#### 4.13. TUNEL Assay

After 30 min of 0.1% Triton X-100 incubation, tumor slices underwent two PBS washes. The TUNEL assay was carried out following the kit's directions. Slices were photographed under a microscope after the nuclei were stained with DAPI for 10 min at room temperature.

#### 4.14. Immunohistochemistry

An immunohistochemical assay was performed to evaluate the amount of Ki67. Lung sections were briefly deparaffinized by xylene and rehydrated before being submerged in the antigen retrieval solutions for 15 min. After samples were exposed to the Ki67 antibody at 4 °C for overnight incubation, they were then exposed to the secondary antibody for an additional hour. Following that, the kit's instructions (Sangon Biotech, Shanghai, China) called for immunohistochemistry detection. Finally, a microscope was used to view the stained slices.

#### 4.15. Statistical Analysis

The information was displayed as means and standard deviations. The statistical significance was examined using Student's *t*-test. Statistical significance was indicated by a *p* value of 0.05 or lower.

### 5. Conclusions

Overall, we successfully developed an efficient and safe delivery system of chitosan-based cationic nanoemulsions for the co-delivery of XIAP-siRNA and GA. The system can synergistically promote tumor cell apoptosis and inhibit the malignant proliferation of lung tumors. Chitosan imparts a positive charge and biocompatibility to a co-delivery system for better siRNA protection and rapid drug release into tumor cells. XIAP siRNA can not only promote cell apoptosis but also inhibit the proliferation of tumor cells by regulating the cell cycle. *In vivo* studies showed that GA-SNE significantly inhibited tumor growth by pulmonary administration and elicited little toxicity in mice. According to these results, pulmonary delivery of siRNA and GA treatment using chitosan-based cationic nanoemulsions may be a potential approach to the treatment of lung tumors.

**Author Contributions:** M.X.: Software, Validation, Writing—Original Draft; L.Z.: Formal Analysis, Software; Y.G.: Investigation, Software; L.B.: Investigation, Validation; Y.L.: Project Administration; B.W.: Investigation; M.K.: Investigation; X.L.: Project Administration; M.S.: Investigation; C.W.: Resources; J.X.: Conceptualization. All authors have read and agreed to the published version of the manuscript.

**Funding:** This work was supported by the Natural Science Foundation Project of CQCSTC (No. cstc2021-jcyj-msxmX0382, cstc2021jcyj-msxmX0344); Science and Technology Research Program of Chongqing Municipal Education Commission (Grant No. KJQN202101140); Science and Technology Talents in Banan District of Chongqing (grant number: 2020TJZ018); Scientific Research Foundation of Chongqing University of Technology; Natural Science Foundation Project of CQCSTC (cstc2021jcyj-msxmX0342) and the Graduate Scientific Research and Innovation Foundation of Chongqing, China (No. CYS21072).

**Institutional Review Board Statement:** The animal study protocol was approved by the Institutional Ethics Committee of Chongqing University of Technology (protocol code 202120, 21 June 2021).

**Informed Consent Statement:** Not applicable.

**Data Availability Statement:** Not applicable.

**Acknowledgments:** We thank Teng Lesheng for his suggestions and help with this paper.

**Conflicts of Interest:** The authors declare no conflict of interest.

## Abbreviations

CNE	Cationic nano-emulsion
C6	Coumarin 6
CS	Chitosan
CS-CNE	Chitosan-Cationic nano-emulsion
CS-SNE	Chitosan-siRNA nano-emulsion
DLS	Dynamic light scattering
GA	Gambogic acid
GA-CNE	Gambogic acid-Cationic nano-emulsion
GA-SNE	Gambogic acid-siRNA nano-emulsion
PDI	Polymer dispersity index
XIAP	X-linked Inhibitor of Apoptosis Protein

## References

1. Ferlay, J.; Soerjomataram, I.; Dikshit, R.; Eser, S.; Mathers, C.; Rebelo, M.; Parkin, D.M.; Forman, D.; Bray, F. Cancer incidence and mortality worldwide: Sources, methods and major patterns in GLOBOCAN 2012. *Int. J. Cancer* **2015**, *136*, E359–E386. [[CrossRef](#)] [[PubMed](#)]
2. Jakobsen, J.N.; Sorensen, J.B. Intratumor heterogeneity and chemotherapy-induced changes in EGFR status in non-small cell lung cancer. *Cancer Chemother. Pharmacol.* **2012**, *69*, 289–299. [[CrossRef](#)] [[PubMed](#)]
3. Hirsch, F.R.; Scagliotti, G.V.; Mulshine, J.L.; Kwon, R.; Curran, W.J., Jr.; Wu, Y.L.; Paz-Ares, L. Lung cancer: Current therapies and new targeted treatments. *Lancet* **2017**, *389*, 299–311. [[CrossRef](#)]
4. Lemjabbar-Alaoui, H.; Hassan, O.U.; Yang, Y.W.; Buchanan, P. Lung cancer: Biology and treatment options. *Biochim. Biophys. Acta* **2015**, *1856*, 189–210. [[CrossRef](#)] [[PubMed](#)]
5. Kim, Y.H.; Mishima, M. Maintenance chemotherapy for non-small-cell lung cancer. *Cancer Treat. Rev.* **2011**, *37*, 505–510. [[CrossRef](#)]
6. Wu, L.; Leng, D.; Cun, D.; Foged, C.; Yang, M. Advances in combination therapy of lung cancer: Rationales, delivery technologies and dosage regimens. *J. Control. Release* **2017**, *260*, 78–91. [[CrossRef](#)]
7. Lee, W.H.; Loo, C.Y.; Ghadiri, M.; Leong, C.R.; Young, P.M.; Traini, D. The potential to treat lung cancer via inhalation of repurposed drugs. *Adv. Drug Deliv. Rev.* **2018**, *133*, 107–130. [[CrossRef](#)]
8. Wong, J.; Brugger, A.; Khare, A.; Chaubal, M.; Papadopoulos, P.; Rabinow, B.; Kipp, J.; Ning, J. Suspensions for intravenous (IV) injection: A review of development, preclinical and clinical aspects. *Adv. Drug Deliv. Rev.* **2008**, *60*, 939–954. [[CrossRef](#)]
9. Thanki, K.; van Eetvelde, D.; Geyer, A.; Fraire, J.; Hendrix, R.; Van Eygen, H.; Putteman, E.; Sami, H.; de Souza Carvalho-Wodarz, C.; Franzzyk, H.; et al. Mechanistic profiling of the release kinetics of siRNA from lipidoid-polymer hybrid nanoparticles in vitro and in vivo after pulmonary administration. *J. Control. Release* **2019**, *310*, 82–93. [[CrossRef](#)]
10. Li, Z.; Wang, Y.; Shen, Y.; Qian, C.; Oupicky, D.; Sun, M. Targeting pulmonary tumor microenvironment with CXCR4-inhibiting nanocomplex to enhance anti-PD-L1 immunotherapy. *Sci. Adv.* **2020**, *6*, eaaz9240. [[CrossRef](#)]

11. Kuzmov, A.; Minko, T. Nanotechnology approaches for inhalation treatment of lung diseases. *J. Control. Release* **2015**, *219*, 500–518. [[CrossRef](#)] [[PubMed](#)]
12. Banik, K.; Harsha, C.; Bordoloi, D.; Laldhuksaki Sailo, B.; Sethi, G.; Leong, H.C.; Arfuso, F.; Mishra, S.; Wang, L.; Kumar, A.P.; et al. Therapeutic potential of gambogic acid, a caged xanthone, to target cancer. *Cancer Lett.* **2018**, *416*, 75–86. [[CrossRef](#)] [[PubMed](#)]
13. Kashyap, D.; Mondal, R.; Tuli, H.S.; Kumar, G.; Sharma, A.K. Molecular targets of gambogic acid in cancer: Recent trends and advancements. *Tumor Biol.* **2016**, *37*, 12915–12925. [[CrossRef](#)] [[PubMed](#)]
14. Liu, Y.; Chen, Y.; Lin, L.; Li, H. Gambogic Acid as a Candidate for Cancer Therapy: A Review. *Int. J. Nanomed.* **2020**, *15*, 10385–10399. [[CrossRef](#)]
15. Sang, M.M.; Liu, F.L.; Wang, Y.; Luo, R.J.; Huan, X.X.; Han, L.F.; Zhang, Z.T.; Feng, F.; Qu, W.; Liu, W.; et al. A novel redox/pH dual-responsive and hyaluronic acid-decorated multifunctional magnetic complex micelle for targeted gambogic acid delivery for the treatment of triple negative breast cancer. *Drug Deliv.* **2018**, *25*, 1846–1857. [[CrossRef](#)]
16. Liang, H.; Zhou, Z.; Luo, R.; Sang, M.; Liu, B.; Sun, M.; Qu, W.; Feng, F.; Liu, W. Tumor-specific activated photodynamic therapy with an oxidation-regulated strategy for enhancing anti-tumor efficacy. *Theranostics* **2018**, *8*, 5059–5071. [[CrossRef](#)]
17. Danson, S.; Dean, E.; Dive, C.; Ranson, M. IAPs as a target for anticancer therapy. *Curr. Cancer Drug Targets* **2007**, *7*, 785–794. [[CrossRef](#)]
18. Cheung, C.H.A.; Chang, Y.C.; Lin, T.Y.; Cheng, S.M.; Leung, E. Anti-apoptotic proteins in the autophagic world: An update on functions of XIAP, Survivin, and BRUCE. *J. Biomed. Sci.* **2020**, *27*, 31. [[CrossRef](#)]
19. Abbas, R.; Larisch, S. Targeting XIAP for Promoting Cancer Cell Death-The Story of ARTS and SMAC. *Cells* **2020**, *9*, 663. [[CrossRef](#)]
20. Zhang, H.; Li, Z.; Wang, K.; Ren, P. Combined treatment of XIAP-targeting shRNA and celecoxib synergistically inhibits the tumor growth of nonsmall cell lung cancer cells in vitro and in vivo. *Oncol. Rep.* **2015**, *33*, 1079–1088. [[CrossRef](#)]
21. Jiang, C.; Yi, X.P.; Shen, H.; Li, Y.X. Targeting X-linked inhibitor of apoptosis protein inhibits pancreatic cancer cell growth through p-Akt depletion. *World J. Gastroenterol.* **2012**, *18*, 2956–2965. [[CrossRef](#)]
22. Ma, J.J.; Chen, B.L.; Xin, X.Y. XIAP gene downregulation by small interfering RNA inhibits proliferation, induces apoptosis, and reverses the cisplatin resistance of ovarian carcinoma. *Eur. J. Obstet. Gynecol. Reprod. Biol.* **2009**, *146*, 222–226. [[CrossRef](#)] [[PubMed](#)]
23. Yuan, Z.Q.; Chen, W.L.; You, B.G.; Liu, Y.; Yang, S.D.; Li, J.Z.; Zhu, W.J.; Zhou, X.F.; Liu, C.; Zhang, X.N. Multifunctional nanoparticles co-delivering EZH2 siRNA and etoposide for synergistic therapy of orthotopic non-small-cell lung tumor. *J. Control. Release* **2017**, *268*, 198–211. [[CrossRef](#)] [[PubMed](#)]
24. Norouzi, P.; Motasadzadeh, H.; Atyabi, F.; Dinarvand, R.; Gholami, M.; Farokhi, M.; Shokrgozar, M.A.; Mottaghitalab, F. Combination Therapy of Breast Cancer by Codelivery of Doxorubicin and Survivin siRNA Using Polyethylenimine Modified Silk Fibroin Nanoparticles. *ACS Biomater. Sci. Eng.* **2021**, *7*, 1074–1087. [[CrossRef](#)] [[PubMed](#)]
25. Lee, J.; Cho, Y.J.; Lee, J.W.; Ahn, H.J. KSP siRNA/paclitaxel-loaded PEGylated cationic liposomes for overcoming resistance to KSP inhibitors: Synergistic antitumor effects in drug-resistant ovarian cancer. *J. Control. Release* **2020**, *321*, 184–197. [[CrossRef](#)]
26. Zhang, W.; Zhou, H.; Yu, Y.; Li, J.; Li, H.; Jiang, D.; Chen, Z.; Yang, D.; Xu, Z.; Yu, Z. Combination of gambogic acid with cisplatin enhances the antitumor effects on cisplatin-resistant lung cancer cells by downregulating MRP2 and LRP expression. *Onco Targets Ther.* **2016**, *9*, 3359–3368. [[CrossRef](#)]
27. Zhang, H.; Li, M.; Zhang, J.; Shen, Y.; Gui, Q. Exosomal Circ-XIAP Promotes Docetaxel Resistance in Prostate Cancer by Regulating miR-1182/TPD52 Axis. *Drug Des. Dev. Ther.* **2021**, *15*, 1835–1849. [[CrossRef](#)]